Available online at www.sciencedirect.com
SCIENCE DIRECT
Journal of Magnetic Resonance 180 (2006) 210–221
JMR Journal of Magnetic Resonance
www.elsevier.com/locate/jmr

^{1}H–^{13}C INEPT MAS NMR correlation experiments with ^{1}H–^{1}H mediated magnetization exchange to probe organization in lipid biomembranes

T.M. Alam *, G.P. Holland

Department of Electronic and Nanostructured Materials, Sandia National Laboratories, Albuquerque, NM 87185, USA

Received 14 December 2005; revised 18 February 2006
Available online 24 March 2006

Abstract

Two-dimensional ^{1}H–^{13}C INEPT MAS NMR experiments utilizing a ^{1}H–^{1}H magnetization exchange mixing period are presented for characterization of lipid systems. The introduction of the exchange period allows for structural information to be obtained via ^{1}H–^{1}H dipolar couplings but with ^{13}C chemical shift resolution. It is shown that utilizing a RFDR recoupling sequence with short mixing times in place of the more standard NOE cross-relaxation for magnetization exchange during the mixing period allowed for the identification and separation of close ^{1}H–^{1}H dipolar contacts versus longer-range inter-molecular ^{1}H–^{1}H dipolar cross-relaxation. These 2D INEPT experiments were used to address both intra- and inter-molecular contacts in lipid and lipid/cholesterol mixtures.

Keywords: INEPT; HETCOR; MAS NMR; Biomembranes; RFDR; lipids

1. Introduction

Magic angle spinning (MAS) NMR continues to be an important and versatile tool for the investigation of lipids and biological membranes. Investigations using ^{1}H, ^{13}C, ^{31}P, and ^{14}N MAS NMR on a variety of different lipid and membrane systems has been reported [1–8]. Due to the high sensitivity ^{1}H was one of the first nuclei pursued using modern MAS NMR techniques [9,10]. It has been found that the rapid axial rotation, fast lateral diffusion and *trans-gauche* isomerizations of the lipids in the liquid crystalline (L_{α}) phase significantly averages the ^{1}H–^{1}H dipolar coupling transforming the interaction from homogeneous to inhomogeneous such that modest spinning speeds can produce well resolved ^{1}H MAS spectra [10–12]. These observations prompted a series of two-dimensional (2D) ^{1}H NOESY MAS NMR experiments that allowed molecular contacts between different lipid regions, as well as between lipids and other constituents within the membrane to be determined [13–18]. The observation of contacts between the methyl protons in lipid headgroup and the protons of the terminal methyl in the alkyl chain lead to extensive discussion into the relative impact of spin diffusion and intermolecular dipolar interactions resulting from lipid disorder on the observed cross-relaxation in ^{1}H NOESY MAS NMR experiments [13,14,17,19,20]. More recently, the selectivity and sensitivity of ^{1}H MAS NMR has been improved by use of pulsed field gradients (PFG) [2]. The use of gradients and ^{1}H MAS NMR has also allowed the measurement of diffusion rates in lipid and biomembranes systems [21–23], while ^{1}H saturation transfer experiments probing specific lipid–protein interactions have been recently reported [24]. A common limitation or difficulty encountered in many of these ^{1}H MAS NMR studies is the severe spectral overlap between different lipids and sterol constituents in complex membrane systems.

To improve the spectral resolution 2D ^{1}H–^{13}C MAS NMR correlation experiments have also been developed

* Corresponding author. Fax: +1 505 844 9624.
E-mail address: tmalam@sandia.gov (T.M. Alam).

1090-7807/$ - see front matter © 2006 Elsevier Inc. All rights reserved.
doi:10.1016/j.jmr.2006.02.013

for lipid systems, including ^{1}H-presaturation cross polarization (CP) transfer experiments and CP based heteronuclear correlation (HETCOR) experiments [7,8,25–27]. The effectiveness and variation of the CP transfer was used to estimate ^{13}C–^{1}H, ^{31}P–^{1}H, and ^{31}P–^{13}C dipolar couplings as a basis for structural input. 2D ^{1}H–^{13}C dipolar recoupling experiments have also been developed to directly measure CH dipolar order parameters [28,29], or inter-proton dipolar pair order parameters [30]. For lipid systems higher MAS frequencies can effectively reduce residual ^{1}H–^{1}H dipolar interactions such that *J*-coupling polarization transfer experiments become feasible. It has been shown that the ^{1}H–^{13}C INEPT (Insensitive Nuclei Enhancement by Polarization Transfer) experiment under MAS is well suited for lipid systems in the L_α phase [6]. The INEPT experiment has the advantage that the ^{1}H–^{13}C polarization transfer occurs directly through the CH bond via *J*-coupling such that non-bonding correlations are not observed, and is independent of the CH bond orientation. The efficiency of the ^{1}H–^{13}C INEPT transfer has also been shown to be sensitive to the motional dynamics of the different ^{1}H environments, and can be used as a probe of different lipid phases [12]. The INEPT experiment is easily incorporated into 2D ^{1}H–^{13}C HETCOR experiments and has been reported for uniformly labeled lipid dispersions [31] and lipid–cholesterol mixtures [7,32,33]. 2D gradient enhanced ^{1}H–^{13}C HSQC (Heteronuclear Single Quantum Coherence) MAS NMR experiments have also been reported for dimyristoylphosphatidylcholine (DMPC)/cholesterol mixtures allowing for the complete assignment of cholesterol in the lipid L_α phase [32,33].

In this paper, we extend these 2D ^{1}H–^{13}C INEPT MAS NMR correlation experiments by introducing a mixing period for ^{1}H spin exchange to probe intra- and inter-molecular ^{1}H–^{1}H contacts within model lipid systems. This type of experiment was originally demonstrated by Alonoso and Massiot for mesostructured materials at very high spinning speeds [34]. Two different schemes for ^{1}H–^{1}H dipolar magnetization exchange where investigated. The first scheme used a mixing period with no ^{1}H irradiation during the mixing period corresponding to standard incoherent dipolar NOESY cross-relaxation, and a second scheme used a radio-frequency dipolar recoupling (RFDR) pulse sequence during the mixing period to coherently drive the ^{1}H–^{1}H magnetization exchange. Examples of the 2D ^{1}H–^{13}C INEPT MAS correlation experiment on pure DMPC and DMPC/cholesterol mixture are presented and discussed.

2. Experimental

Unlabelled 1,2-dimyristoyl-*sn*-glycero-3-phosphocholine (DMPC), [1,2-$^{2}H_{54}$]-dimyristoyl-*sn*-glycero-3- phosphocholine (DMPC-d_{54}) and unlabelled cholesterol (CHOL) were purchased from Avanti Polar Lipids (Alabaster, AL). Multilamellar vesicles (MLV) were prepared by dissolving a 1:1 mol% mixture of lipid and cholesterol in chloroform/methanol (3:1 v/v). Samples were then dried overnight under vacuum, and suspended in de-ionized water to produce a 28 wt% DMPC concentration. This mixture was then freeze–thawed–centrifuged 5 times. The lipid samples were transferred to 4 mm zirconia MAS rotors and sealed with kel-F inserts and caps. No dehydration effects were observed. The typical volume of MLV sample for NMR analysis was 50–100 μL corresponding to 25–50 mg of phospholipid. The samples were stored in a −20 °C freezer when NMR experiments were not being performed.

All NMR experiments were performed on a Bruker Avance 600 spectrometer at an observe frequency of 600.14 and 150.92 MHz for ^{1}H and ^{13}C, respectively. The 1D ^{1}H MAS NMR spectra were obtained using 8 K points with a 30 kHz spectral width. The 1D ^{13}C CPMAS and ^{1}H–^{13}C INEPT spectra were obtained using 4 K points with a 42 kHz spectral width. All ^{13}C and ^{1}H chemical shifts were referenced to the C-14 ($\delta = +14.0$ ppm) and H-14 ($\delta = +0.9$ ppm) resonances of DMPC [35]. The experiments utilized a 4 mm broadband MAS NMR probe with sample temperatures maintained at ±0.2 K through the regulation of the bearing N_2 temperature. Heating effects due to frictional heating during sample spinning and due to rf irradiation during ^{1}H decoupling have previously been discussed [35]. These heating effects at moderate spinning speeds and high decoupling powers are not negligible, but can be compensated for appropriate choice of decoupling powers, spinning speed, and "set" temperatures. In the present study, actual sample temperatures were calibrated using the ^{1}H chemical shift difference ($\Delta\delta$) between the H-14 and H_2O resonances as detailed by Dvinskikh and co-workers [35]. A 2 K increase in the lipid sample temperature was observed for a 5 kHz spinning speed, while a 10 kHz spinning speed produced a 10 K increase in sample temperature, versus non-spinning conditions. All temperatures reported in the text are the actual sample temperature determined by this calibration method.

The ^{1}H–^{13}C INEPT MAS NMR correlation experiment [7] modified for ^{1}H–^{1}H mediated magnetization exchange is shown in Fig. 1. The phase cycle for this modified sequence has previously been described [34]. Phase sensitive detection in t_1 was obtained using the States method [36]. All inter-pulse delays (t_1, τ_{mix}, Δ_1 and Δ_2) were rotor synchronized. The delays Δ_1 and Δ_2 were optimized as detailed in the results section. For the ^{1}H–^{13}C correlation experiments presented in this paper, two different methods for ^{1}H–^{1}H magnetization exchange during the mixing time (τ_{mix}) were investigated. In one set of experiments no additional ^{1}H rf pulses were introduced during τ_{mix} such that the observed ^{1}H–^{1}H magnetization exchange occurs via NOE type dipolar relaxation analogous with the ^{1}H NOESY MAS NMR experiments previously reported [13,14,17,19,20]. In the second set of experiments the ^{1}H–^{1}H magnetization exchange occur via scaled ^{1}H–^{1}H dipolar interactions reintroduced using the radio-frequency dipolar recoupling

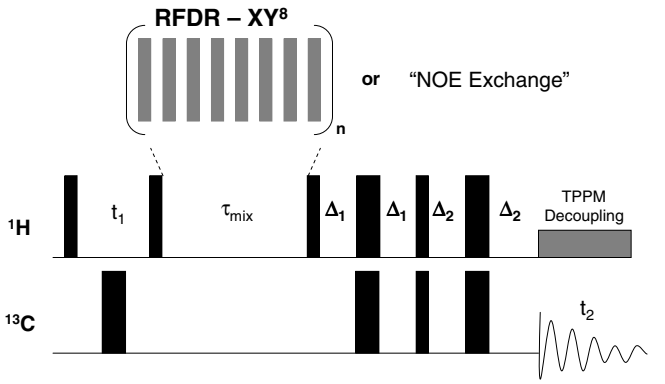

Fig. 1. Two-dimensional refocused ^{1}H–^{13}C INEPT pulse sequence for correlation experiments where a mixing time τ_m is introduced that allows the transfer of magnetization via ^{1}H–^{1}H dipolar interactions either through NOE cross relaxation (no ^{1}H irradiation during τ_m) or recoupled dipolar interactions using a RFDR sequence. In this sequence all t_1, Δ_1, and Δ_2 delays were rotor synchronized ($= n\tau_R = n/\nu_R$, where ν_R is the spinning frequency), and were optimized as described in the text. The phase cycle for this sequence has been previously given [34].

(RFDR) pulse sequence on the ^{1}H channel during τ_{mix}. This sequence consists of rotor-synchronized π pulses with the XY-8 phase cycle to reduce the impact of resonance offsets and pulse errors [37–39]. A 25 kHz TPPM ^{1}H decoupling with a 15° phase shift was used during acquisition [40]. Typical acquisition parameters for the ^{1}H–^{13}C INEPT MAS NMR correlation experiments were 256 scans, 2 s recycle delay, 4 k t_2 points using a 42 kHz spectral width, 64–128 t_1 increments with a 15 kHz spectra width, with spinning speeds ranging from 5 to 10 kHz.

3. Results and discussion

The ^{1}H–^{13}C INEPT polarization transfer sequence for lipid biomembranes has been demonstrated by a number of groups [6,7,12,29,31–33]. These examples have utilized the INEPT sequence for obtaining 1D ^{13}C MAS NMR spectra, or have utilized the INEPT building block in more complicated pulse sequences. The ^{1}H–^{13}C INEPT MAS NMR spectra for the different DMPC and DMPC/CHOL mixtures in the present study are shown in Fig. 2. The ^{13}C NMR resonance assignments for DMPC and cholesterol were based on previous studies (correcting for differences in referencing) [7,27,32,33,35], the sign of the INEPT signal modulation, direct polarization ^{13}C MAS NMR spectra and ^{1}H–^{13}C chemical shift correlations (see below). The assignment of DMPC is given in Fig. 2A, with select cholesterol resonances being shown in Figs. 2B and C. With the addition of 50% cholesterol, the DMPC ^{13}C NMR resonances were not observed to shift significantly (±0.1 ppm) except for the C4–C11 resonance envelope which shifts downfield and narrows slightly (Fig. 2B), consistent with previous investigations [10,41]. The C1 carbonyl resonance has been reported to vary with cholesterol concentration, but that ^{13}C NMR resonance ($\delta = 173.5$ ppm) is not observed in the ^{1}H–^{13}C INEPT experiments since there is

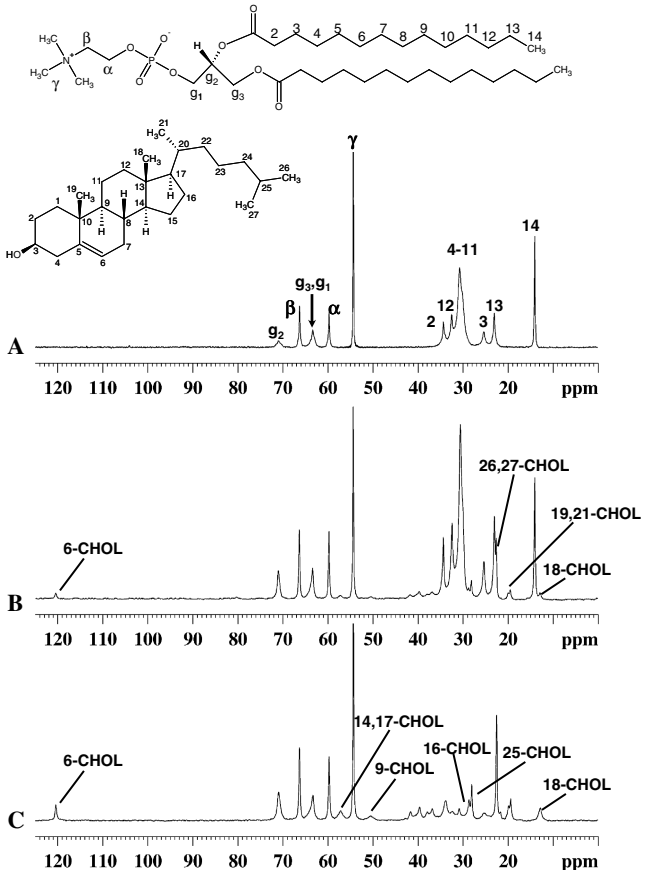

Fig. 2. Refocused ^{1}H–^{13}C INEPT MAS NMR spectra for D_2O dispersion of (A) DMPC, $\nu_R = 7.5$ kHz, $\Delta_1 = 2.1$ ms, $\Delta_2 = 0.66$ ms, 308 K (corrected for spinning/decoupling heating effects) (B) 1:1 DMPC/CHOL, $\nu_R = 7.5$ kHz, $\Delta_1 = 2.1$ ms, $\Delta_2 = 1.2$ ms, 308 K, and (C) DMPC-d_{54}/CHOL, $\nu_R = 10$ kHz, $\Delta_1 = 2.1$ ms, $\Delta_2 = 1.1$ ms, 313 K. The assignment numbering is shown in the molecular scheme, with the resonance assignments for DMPC given in (A) and select resonance assignments for cholesterol given in (B) and (C).

no one bond CH J-coupling present for that resonance, as well as the C5 and C13 carbons of cholesterol.

Fig. 2 also shows that there are differences in the relative intensities between different DMPC carbon environments in the ^{1}H–^{13}C INEPT MAS NMR spectra that depend on the choice of the inter-pulse delays Δ_1 and Δ_2. For example, compare the C3 and C13 resonances of the alkyl chain or the α and β headgroup resonances of DMPC in Figs. 2A and B. The majority of these intensity variations result from different J_{CH} coupling values making the optimization of the INEPT delays resonance specific (see below). More striking is the reduction in the cholesterol resonance intensity in comparison to the phospholipid signal intensity for the ^{1}H–^{13}C INEPT spectra shown in Fig. 2B. This intensity discrepancy is not simply due to differences in the magnitude of J_{CH} couplings; the C18–CHOL and C14 DMPC methyl groups have almost identical J_{CH} but reveal large differences in signal intensity (Fig. 2B). Rather these intensity changes are a function of molecular motions and the degree of ^{1}H–^{1}H dipolar coupling averaging. The impact of this averaging can be seen

in Fig. 2C where the increased spinning speed (and slightly higher temperature) increases the observed intensity of the cholesterol resonances. It is known that saturated phosphatidylcholines (such as DMPC) and cholesterol form a liquid ordered (l_o) phase at higher cholesterol concentrations [42,43]. The addition of cholesterol to DMPC has also been shown to increase the axial rotation rate for the phospholipid, while the rotation of the cholesterol remains significantly slower than that of the lipid [44]. Discussion about the INEPT MAS sequence performance and the impact of differential motional dynamics of lipids and lipid constituents in membrane systems has been limited, except for the recent work by Warschawski and Devaux [12] using INEPT/NOE ratios as a tool to probe different lipid domains. A brief discussion of the optimization of the INEPT sequence for membrane systems is therefore warranted.

3.1. Optimization of the INEPT sequence

In solution the optimization of the INEPT sequence is realized by matching of the Δ_1 and Δ_2 inter-pulse delays (Fig. 1) to coherence evolution under specific values of the J_{CH} coupling. These inter-pulse delays are typically on the order of 1–2 ms. However for rigid solids this can be significantly longer than the ^{1}H transverse relaxation times (T_2^H). For short T_2^H values, the optimal signal intensity observed using the INEPT sequence may no longer correspond to the simple $1/J_{CH}$ relationship. Recent ^{1}H–^{13}C INEPT MAS NMR experiments in mesostructured materials demonstrate that the contributions from T_2^H relaxation need to be directly considered [34]. Assuming that the ^{1}H relaxation (T_2^H) dominates relaxation effects from the ^{13}C (T_2^C), the signal intensity $S(\Delta_1,\Delta_2)$ during the ^{1}H–^{13}C INEPT experiment is given by [34,45]

$$
\begin{aligned}
&S(\Delta_1,\Delta_2) \sim F_1(\Delta_1,T_2^H)F_2(\Delta_2,T_2^H)\\
&F_1 = \sin(2\pi J_{CH}\Delta_1)\exp[-2\Delta_1/T_2^H]\\
&F_2 = \sin(2\pi J_{CH}\Delta_2)\exp[-2\Delta_2/T_2^H], AX\\
&F_2 = \sin(4\pi J_{CH}\Delta_2)\exp[-2\Delta_2/T_2^H], AX_2\\
&F_2 = \frac{3}{4}\{\sin(2\pi J_{CH}\Delta_2)\sin(6\pi J_{CH}\Delta_2)\}\exp[-2\Delta_2/T_2^H], AX_3,
\end{aligned}
\tag{1}
$$

where the delays Δ_1 and Δ_2 are defined in Fig. 1. The optimal signal intensity is observed at $\Delta_1 \sim 1/4J_{CH}$ and $\Delta_2 \sim 1/4J_{CH}$ for CH, $1/8J_{CH}$ for CH_2, and $\sim 0.098/J_{CH}$ for CH_3.

The question arises are there situations in membrane systems where short T_2^H make a significant impact on the performance of the ^{1}H–^{13}C INEPT sequence? Fig. 3 shows the signal variation of the ^{1}H–^{13}C INEPT MAS NMR sequence as a function of the inter-pulse delays Δ_1 and Δ_2 for select carbon resonances in DMPC at 313 K, $\nu_R = 10$ kHz. The dashed and solid lines were obtained by fitting the experimental results to Eq. (1). The J_{CH} values ranged from 110 to 150 Hz, with the T_2^H values ranging from 15 to 100 ms, consistent with independent T_2 values observed from rotor-synchronized ^{1}H Hahn echo experiments (data not shown). Similar INEPT response curves were observed for the cholesterol resonance, but at a significantly lower relative intensity (see additional discussion below). The long T_2^H values means that the maximum of the signal intensity is not shifted considerably away from the simple theoretical predictions, yet there is a noticeable loss of signal intensity for the longer Δ durations, in particular for Δ_2 values >2 ms, as might be used in experiments to distinguish CH_2 from CH or CH_3 carbon environments.

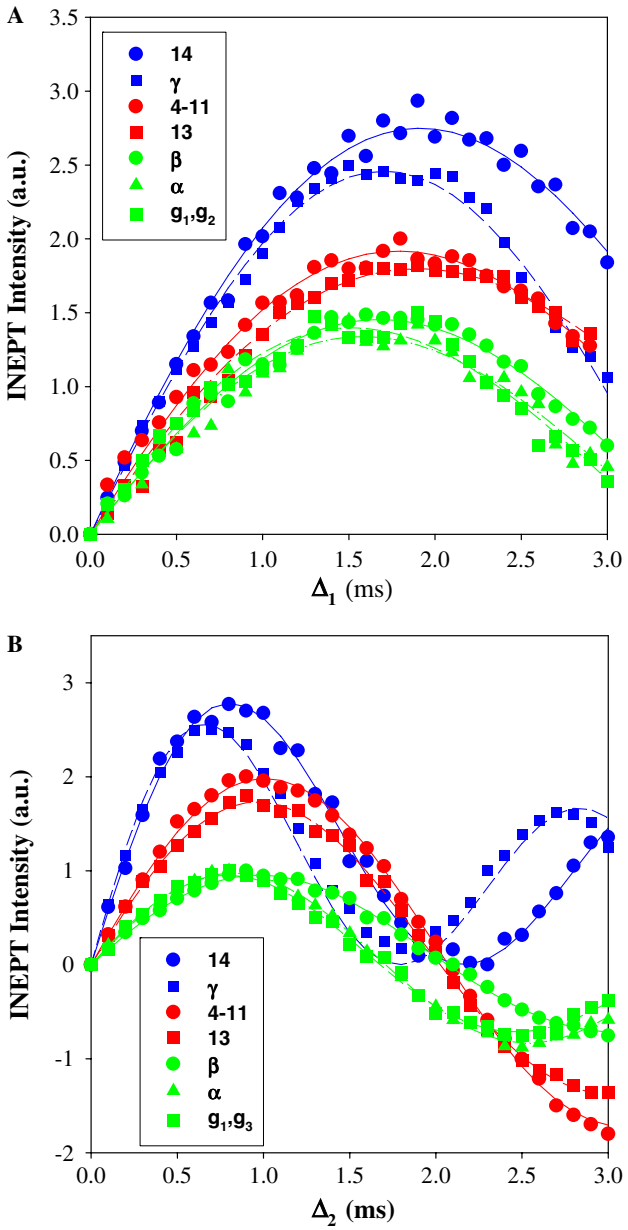

Fig. 3. Signal amplitude variation for the ^{1}H–^{13}C INEPT MAS NMR experiment for a D_2O dispersion of DMPC at 313 K, $\nu_R = 10$ kHz, as a function of the inter-pulse delay Δ_1 and Δ_2. (A) Δ_1 was varied while Δ_2 was held constant at 0.93 ms, while in (B) Δ_1 was kept constant at 2.0 ms and Δ_2 varied. The simulated lines were obtained using Eq. (1). The signal intensities of the different groupings were scaled to improve readability.

For the CH_2 carbons this loss is on the order of 50% and can be related to the shorter T_2^H values observed for the methylene protons. This difficulty in T_2^H related signal loss during long Δ values was noted in the reduced signal noise of methylene carbon resonances in previous studies of DMPC/CHOL [33].

These relatively long T_2^H values and well behaved INEPT signal response agree with the small spinning sideband pattern observed in the ^{1}H MAS NMR spectra of DMPC and DMPC/CHOL shown in Fig. 4, which give a measure of the residual ^{1}H–^{1}H dipolar coupling present. In the ^{1}H MAS NMR spectra of these lipid samples (Fig. 4A) the headgroup resonances of DMPC shows very small ±1 spinning sidebands (relative intensity ~2% of the central isotropic intensity), and almost no higher-order spinning sidebands. The large methylene proton resonance ($\delta = +1.3$ ppm, H4–H13) shows both ±1 and ±2 spinning sidebands, but the +1 sideband constitutes only ~9% of the central intensity at $\nu_R = 7.5$ kHz. Similar results are observed for lipid resonances in the DMPC/CHOL mixture. This observation is consistent with previous studies that reveal that for DMPC in the L_α phase the molecular dynamics are significant, reducing the ^{1}H–^{1}H homonuclear dipolar coupling so that it becomes effectively inhomoge-

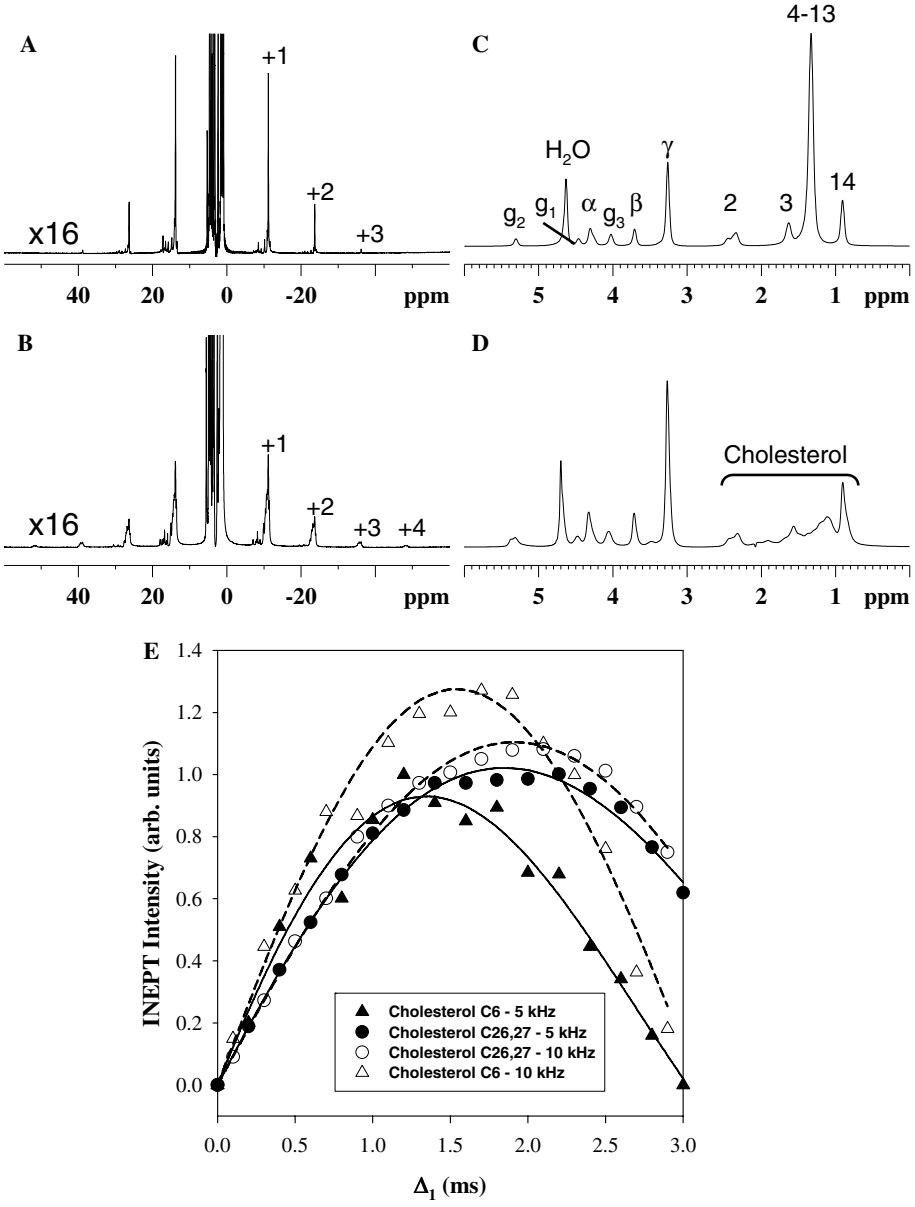

Fig. 4. The ^{1}H MAS NMR spectra of (A) DMPC and (B) DMPC-d_{54}/CHOL at 308 K and $\nu_R = 7.5$ kHz, showing the full spectral window with the different spinning sidebands marked. Expansion of the isotropic spectral region for (C) DMPC, and (D) DMPC-d_{54}/CHOL, with the assignment of the different ^{1}H resonances in DMPC. The variation (E) of the ^{1}H–^{13}C INEPT signal intensity for the C26/C27 methyl resonances ($\delta = +22.6$ ppm) and the C6 methine ($\delta = +120.4$ ppm) cholesterol carbon resonances as a function of spinning speed: cholesterol C26/C27 at 5 kHz (●) and 10 kHz (○) and C6 at 5 kHz (▲) and 10 kHz (△).

neous in nature [9,10,12]. With this motional averaging the T_2^H values become sufficiently long as to not greatly impact the optimization of the INEPT sequence.

Figs. 4B and D shows the ^{1}H MAS NMR spectra of the DMPC-d_{54}/CHOL sample in which many of the cholesterol ^{1}H resonances are now clearly visible. The cholesterol ^{1}H resonances (specifically between $\delta = +0.5$ and $+2.5$ ppm) have a significantly larger spinning sideband manifold, with the intensity of the +1 sideband being ~14%, the +2 sideband 6%, and the +3 sideband 1%, of the central intensity, implying a larger residual ^{1}H–^{1}H dipolar coupling due to the reduced motion of this cholesterol within the membrane. The relative ratio of the spinning sidebands also decreases with increased spinning from $I_{+1}/I_0 \sim 14\%$ at $\nu_R = 7.5$ kHz to $I_{+1}/I_0 \sim 3\%$ at $\nu_R = 12.5$ kHz. Analysis of ^{1}H–^{1}H double quantum (DQ) MAS NMR sideband patterns have revealed residual ^{1}H–^{1}H dipolar couplings (under MAS) between 1 and 4 kHz in related lipid/CHOL mixtures (Alam, personal communication, Rocky Mountain Conference 2005). The apparent proton T_2 as measured from rotor-synchronized Hahn-echo experiments (data not shown) also increases with higher spinning speed suggesting that the INEPT performance should be spinning speed dependent. This is confirmed in Fig. 4E which shows the signal intensity for the ^{1}H–^{13}C INEPT MAS NMR experiment for the C26/C27 methyl resonances ($\delta = +22.6$ ppm) and the C6 methine ($\delta = +120.4$ ppm) carbon resonances of cholesterol. The most important observation was the dramatic increase in the overall signal intensity with increasing spinning speed, especially for the C6 resonance. For these experiments the set temperature was adjusted such that the true sample temperature was the same (308 K) for all the different spinning speeds investigated. For the methyl C26/C27 carbon resonance there was a small ~10% increase in the signal intensity by increasing the spinning speed from 5 to 10 kHz. The T_2^H values obtained from fitting Eq. (1) were ~50 ms. The rapid internal motion of the methyl group still produces significant averaging of the ^{1}H–^{1}H dipolar coupling that the spinning speed variation is minor. For the cholesterol C6 methine carbon environment increasing the spinning speed from 5 and 10 kHz produced an >25% increase in the overall signal intensity. The corresponding T_2^H values was found to be ~10 ms. For the less mobile sterol component the efficiency of the INEPT sequence is dramatically reduced by the increased ^{1}H–^{1}H dipolar coupling, but a portion of this impact can be reduced by increases in the spinning rate. This is also consistent with the slower axial rotation observed for cholesterol in comparison to DMPC based on ^{2}H NMR relaxation studies [44]. Unfortunately, ultra-high spinning speeds (>20 kHz) readily applied to other materials are not applicable to membrane systems due to the segregation/centrifugation of the water from the lipid mixture. These results presented above can now be used for the optimization of the 2D ^{1}H–^{13}C INEPT MAS NMR correlation experiments described below.

3.2. Two-dimensional ^{1}H–^{13}C heteronuclear correlation

The 2D ^{1}H–^{13}C INEPT MAS NMR heteronuclear correlation spectrum for DMPC at a short mixing time ($\tau_{mix} = 1$ ms) is shown in Fig. 5 (total experiment time ~4.5 h), while the 2D correlation spectrum for DMPC-d_{54}/cholesterol is shown in Fig. 6. These results show that these heteronuclear correlation experiments at natural ^{13}C abundance can readily be performed. The benefit of the INEPT experiment is that the correlations arise from direct bonding interactions through the J_{CH} coupling polarization transfer, and do not contain cross peaks due to long range interactions as well as being independent of the CH bond orientation. The C1 carbonyl region, $\delta(^{13}C) = +173.5$ ppm, is not shown since no cross peaks will be observed in the INEPT experiments for quaternary carbon environments. These 2D spectra allow confirmation of ^{1}H and ^{13}C resonance assignments and are consistent with previous investigations [13,33,35]. The 2D ^{1}H–^{13}C INEPT MAS NMR correlation spectrum for the DMPC/CHOL mixture (data not shown) is similar to Fig. 5 and shows significant overlap between many of the DMPC and cholesterol resonances even in the 2D experiment, but also reveals several distinct cholesterol resonances including the C6 methine at $\delta(^{13}C) = +120.4$ ppm, the C3 methine at $\delta(^{13}C) = +70.7$ ppm, the C14,C17 methines at $\delta(^{13}C) = +57.2$ ppm, the C9 methine at $\delta(^{13}C) = +50.9$ ppm, and the C18 methyl at $\delta(^{13}C) = +12.9$ ppm. By using DMPC-d_{54}/ CHOL mixtures, it is possible to

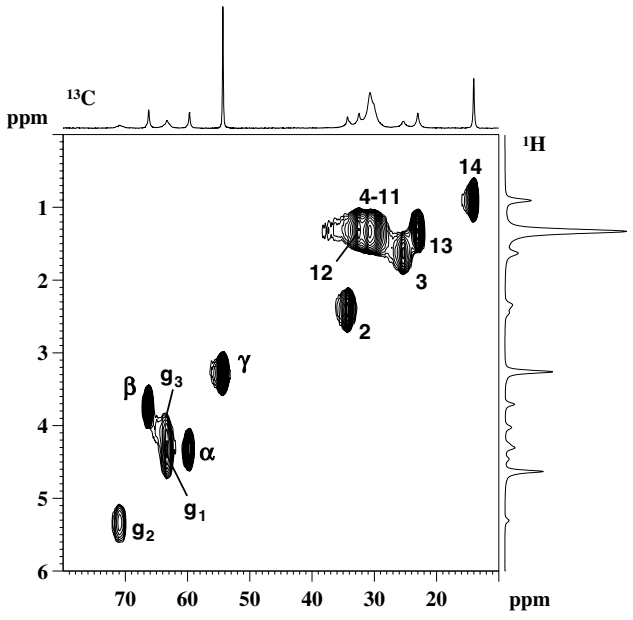

Fig. 5. The 2D ^{1}H–^{13}C INEPT MAS NMR correlation spectra for DMPC obtained using the rotor-synchronized pulse sequence in Fig. 1 at $\nu_R = 7.5$ kHz, 308 K, $\tau_{mix} = 1$ ms, $\Delta_1 = 2.1$ ms, and $\Delta_2 = 0.67$ ms. The DMPC assignments are shown. The ^{13}C and ^{1}H projections are the 1D ^{1}H–^{13}C INEPT MAS and the 1D ^{1}H MAS NMR spectra, respectively. The low resolution in the F1 (^{1}H) dimension results from the reduced number of t_1 increments used to reduce experimental time.

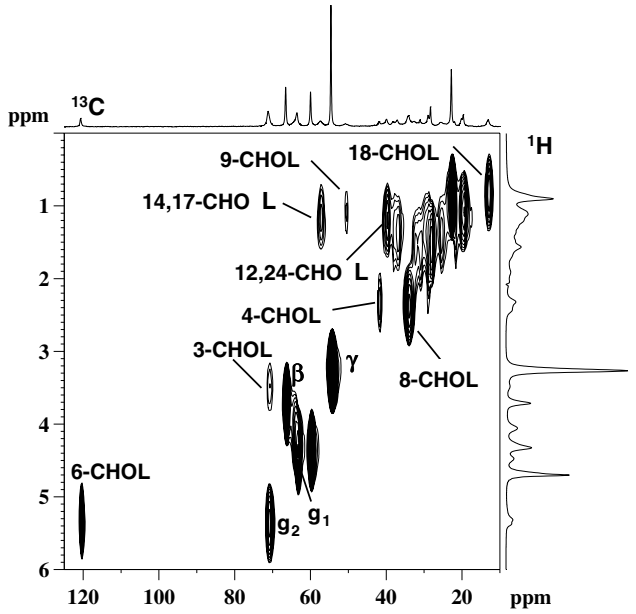

Fig. 6. The 2D ^{1}H–^{13}C INEPT MAS NMR correlation spectra for DMPC-d_{54}/CHOL obtained using the rotor-synchronized pulse sequence in Fig. 1 at $\nu_R = 10$ kHz, 313 K, $\tau_{mix} = 1$ ms, $\Delta_1 = 2.2$ ms, and $\Delta_2 = 1.2$ ms. The undeuterated DMPC headgroup resonances and selective cholesterol assignments are shown. The ^{13}C and ^{1}H projections are the 1D ^{1}H–^{13}C INEPT MAS and the 1D ^{1}H MAS NMR spectra, respectively. The low resolution in the F1 (^{1}H) dimension results from the reduced number of t_1 increments used to reduce experimental time.

observe and identify all proton containing cholesterol carbon resonances as shown in Fig. 6. Again the lipid carbonyl region and the cholesterol C5 quaternary, $\delta(^{13}C) = +142$ ppm, spectral region is not shown since the INEPT experiment does not produce cross peaks for these carbon environments. ^{1}H–^{13}C HETCOR correlation experiments have been reported that utilized ^{13}C–C3,C4 labeled cholesterol in order to emphasize and clearly identify cholesterol cross peaks [7]. The 2D INEPT reported here demonstrate that ^{13}C labeling is not required to obtain correlation experiments in cholesterol containing membrane mixtures. The one draw back of these 2D INEPT experiments is the relatively low ^{1}H resolution afforded by the direct ^{13}C detection. This reduced ^{1}H resolution is clearly seen in the 2D spectra shown Figs. 5 and 6 (compared to the 1D ^{1}H MAS projections) where a very limited number of t_1 increments were used to help reduce overall experimental time. There is also a slight increase in the ^{13}C line width versus the 1D projection as a result of doubling the exponential line broadening for the 2D spectra. More recently, ^{1}H–^{13}C HMQC experiments have been reported for DMPC/CHOL mixtures that overcome this limitation [32,33].

3.3. ^{1}H–^{1}H dipolar cross-relaxation

To explore through space connectivities and interactions the 2D ^{1}H–^{13}C INEPT MAS NMR correlation experiments were expanded (Fig. 1) to include a mixing time (τ_{mix}). During this period no additional *rf* pulses are applied to either channel such that ^{1}H–^{1}H magnetization exchange occurs via dipolar cross-relaxation. These types of experiments are analogous to ^{1}H–^{1}H MAS NOESY experiments [13–18,46] but now include the improved resolution afforded by ^{13}C detection. Similar to the ^{1}H NOESY experiments, ^{1}H–^{1}H correlations only become significant for $\tau_{mix} > 100$ ms. Fig. 7 shows the 2D ^{1}H–^{13}C INEPT MAS NMR correlation spectra at $\tau_{mix} = 300$ ms for DMPC. Numerous cross-peaks are observed (compared to Fig. 5) correlating different ^{1}H environments to a single carbon environments as a result of ^{1}H–^{1}H dipolar cross-relaxation. These include the short range through-space ^{1}H–^{1}H dipolar interactions between g_1 and g_2, g_2 and α, along with g_2 and γ within the DMPC head group, plus the C2–C3 interaction within the alkyl chain. In addition, long range inter-molecular correlations are observed including the dipolar cross-relaxation between γ and 4–11 carbons, γ to the C14 methyl and α to the C14 methyl. These interactions have previously been noted and discussed in the 2D ^{1}H–^{1}H NOESY investigations, [13,14,16,46] and demonstrate the dynamical disorder of the lipid present within the L_α phase. The scaled S/N of this 2D spectrum (scaled for the increased number of acquisitions) is ~30% of that observed in Fig. 5. This S/N merit was estimated from the area of the intense γ resonance, with some loss expected due to relaxation during the 300 ms mixing period, but also reflects some loss of signal due to magnetization exchange with other coupled protons.

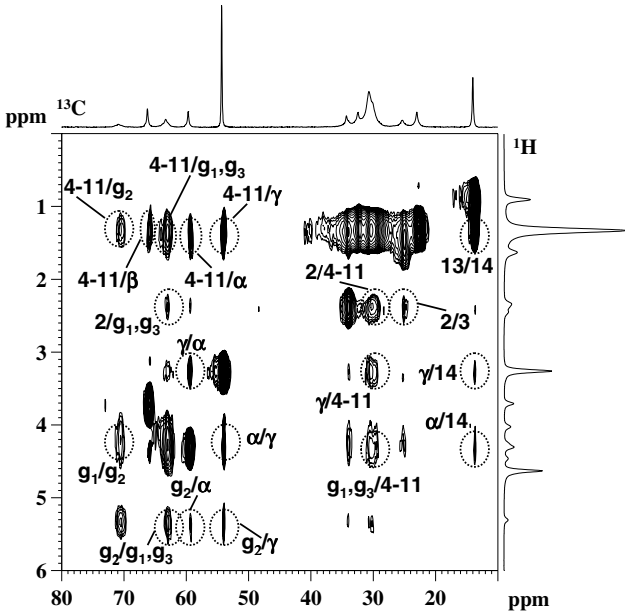

Fig. 7. The 2D ^{1}H–^{13}C INEPT MAS NMR correlation spectra for DMPC obtained using the rotor-synchronized pulse sequence in Fig. 1 at $\nu_R = 7.5$ kHz, 308 K, $\tau_{mix} = 300$ ms, $\Delta_1 = 2.1$ ms, and $\Delta_2 = 0.67$ ms. Selective correlation cross peaks arising from ^{1}H–^{1}H magnetization exchange are labeled. See Fig. 5 for assignment of standard one-bond ^{1}H–^{13}C correlations.

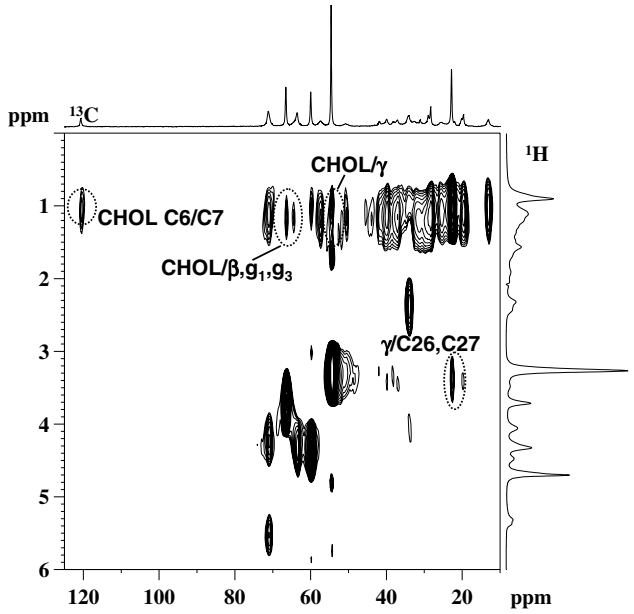

Fig. 8. The 2D ^{1}H–^{13}C INEPT MAS NMR correlation spectra for DMPC-d_{54}/CHOL obtained using the rotor-synchronized pulse sequence in Fig. 1 at $\nu_R = 10$ kHz, 313 K, $\tau_{mix} = 250$ ms, $\Delta_1 = 2.2$ ms, and $\Delta_2 = 1.2$ ms. Selective cholesterol/lipid correlation cross peaks arising from ^{1}H–^{1}H magnetization exchange are labeled. See Fig. 6 for assignment of standard one-bond ^{1}H–^{13}C correlations.

Similarly the 2D ^{1}H–^{13}C INEPT MAS NMR correlation spectrum for the DMPC-d_{54}/CHOL mixture using $\tau_{mix} = 250$ ms is shown in Fig. 8. Again cross peaks between the different carbon resonances are observed (compared to Fig. 6), including dipolar interactions within cholesterol (C6 to C7) as well as lipid–cholesterol interactions including: β, g_1, g_2 contacts to cholesterol, γ to cholesterol, and γ to the C26, C27 methyl carbons of cholesterol. The low ^{1}H dispersion of the cholesterol resonances in the $\delta(^{1}H) = +0.5$ to 1.5 ppm region make the assignment of these lipid–cholesterol contacts to specific cholesterol environments difficult, so we have simply denoted them as cholesterol contacts. From the 1D ^{1}H MAS NMR experiments along with the 1D ^{1}H–^{13}C INEPT (including phase variation with Δ_2, see section of INEPT optimization) we know that there is not a significant contribution from residual non-deuterated lipid in the $\delta(^{1}H) = +0.5$ to 1.5 ppm region, supporting our arguments that the observed contacts are between the lipid and cholesterol. Also the strong ^{1}H–^{13}C cross-peak observed at $\delta(^{13}C) = +33.9$ ppm, $\delta(^{1}H) = +2.4$ ppm in Fig. 6 is assigned to the C8 of cholesterol since the signal modulation observed in 2D INEPT spectra for long Δ_2 values (data not shown) is consistent with a CH or CH_3 carbon environment, and not with a CH_2 species. There is a small contribution from residual non-deuterated C4–C11 methylene CH_2 carbons of the DMPC observed at $\delta(^{13}C) = +34.1$ ppm and $\delta(^{1}H) = +1.3$ ppm, but it is not visible in Fig. 6. It should also be noted that the intensity of cross peaks between the lipid head group resonances in the DMPC-d_{54}/CHOL mixture are lower than observed in pure DMPC (Fig. 7) or DMPC/CHOL mixtures. This reduction is consistent with previous studies that have shown the cross-relaxation occurs via inter-molecular contacts and that the presence of deuterated alkyl chains will slow this process [13,14,46]. These 2D results show that the INEPT correlation experiments can be used to observe inter-molecular contacts between different constituents within membrane mixtures. Again, both Figs. 7 and 8 show a reduced ^{1}H (F1) resolution as a result of the limited number of t_1 increment utilized. The S/N of this 2D spectrum was ~35% of that observed in Fig. 6.

3.4. ^{1}H–^{1}H HRFDR correlation

As discussed above, rapid lateral diffusion in the L_α lipid phase averages intermolecular ^{1}H–^{1}H dipolar interactions, while rapid axial rotation and molecular motions reduces the intra-molecular ^{1}H–^{1}H dipolar interactions within biomembranes. Early, observations that MAS (even at slow spinning speeds) significantly improved the resolution of ^{1}H NMR spectra of membranes showed that residual ^{1}H–^{1}H dipolar couplings were present in these systems. For example, in DMPC (36 °C) and DPPC (50 °C) the dipolar order parameter S_{dip} was measured to be ~0.17 and 0.18, respectively [10]. These MAS-removed ^{1}H–^{1}H dipolar couplings can be reintroduced (scaled) through the use of different multiple pulse dipolar recoupling sequences during the τ_{mix} period (Fig. 1). In the present study, we have utilized the rotor-synchronized radio-frequency dipolar recoupling (RFDR) sequence [37–39,47] to re-introduce residual ^{1}H–^{1}H dipolar coupling via zero-quantum coherences as a means of magnetization transfer [48]. ^{1}H–^{1}H RFDR correlation experiments were recently demonstrated for swollen protein resins [49] and are similar to proton-mediated rare spin correlation experiments developed for protein structure determination in the solid state [50–53]. Fig. 9A shows the 2D ^{1}H–^{13}C INEPT MAS NMR correlation spectrum for DMPC utilizing a $\tau_{mix} = 53.3$ ms RFDR recoupling sequence. This period corresponds to 50 cycles of the XY-8 phase cycle. Even for this relatively short mixing time multiple cross peaks were observed arising from ^{1}H–^{1}H magnetization exchange within the membrane, with the spectrum being very similar to the 300 ms NOESY exchange spectra (Fig. 7). The appearance of ^{1}H–^{1}H correlations at short mixing times distinguishes the RFDR based experiment from the cross-relaxation (NOE) based experiment (Section 3.3) where no significant ^{1}H–^{1}H exchange cross-peaks were observed at $\tau_{mix} = 50$ ms. Using the RFDR significant ^{1}H–^{1}H magnetization exchange was observed for τ_{mix} as short as ~10 ms. For $\tau_{mix} < 50$ ms the appearance of new cross-peaks in the 2D ^{1}H–^{13}C INEPT exchange experiments arise from the coherent reintroduction of dipolar couplings under the RFDR sequence, while for $\tau_{mix} \geqslant 100$ ms ^{1}H–^{1}H magnetization exchange cross-peaks can derive from both the coherent RFDR recoupling and

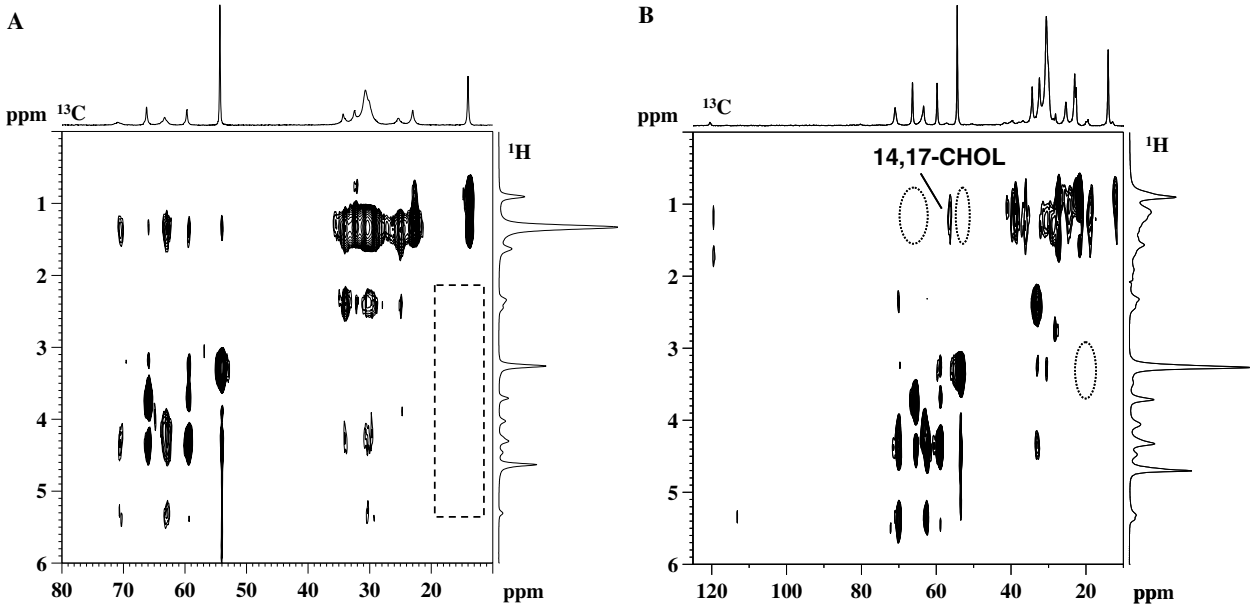

Fig. 9. The 2D ^{1}H–^{13}C INEPT MAS NMR correlation spectra at $\nu_R = 7.5$ kHz, 308 K with RFDR mixing for (A) DMPC at $\tau_{mix} = 53.3$ ms (50 XY-8 recoupling cycles), $\Delta_1 = 2.1$ ms, and $\Delta_2 = 0.67$ ms, and for (B) DMPC-d_{54}/CHOL at $\tau_{mix} = 26.7$ ms (25 XY-8 recoupling cycles), $\Delta_1 = 2.1$ ms, and $\Delta_2 = 1.2$ ms. The dashed boxes and circles mark either missing long range lipid–lipid or cholesterol–lipid ^{1}H–^{1}H magnetization exchange contacts observed in Figs. 7 and 8.

the incoherent (diffusive like) dipolar cross-relaxation. More importantly, the long range inter-molecular dipolar contacts between the headgroup and the alkyl chain are not observed for these short mixing time RFDR type experiments (compare Figs. 7 and 9A, in particular the C14 methyl contacts). The S/N for this 2D spectrum was ~40% of that observed in Fig. 5, but is slightly improved over the S/N obtained from the 300 ms spin exchange experiment shown in Fig. 7. Similar results are observed in the 2D ^{1}H–^{13}C INEPT MAS NMR correlation spectrum for DMPC-d_{54}/CHOL utilizing a $\tau_{mix} = 26.7$ ms RFDR recoupling shown in Fig. 9B, where many of the cholesterol/lipid contacts are not observed due to the reduced magnitude of the inter-molecular dipolar coupling. The one notable exception to this is the cross peak at $\delta(^{13}C) = +33.9$ ppm and $\delta(^{1}H) = +4.3$ ppm (Fig. 9B), which results from contact between the protons of the C8 methine carbon in cholesterol and either the protons of the g_1 or α carbons of the DMPC. As noted above this +33.9 ppm ^{13}C chemical shift originates from a CH or CH_3 carbon species based on INEPT modulation with Δ_2, and is therefore not the residual non-deuterated CH_2 carbons of DMPC. The origin of this strong inter-molecular contact between DMPC and cholesterol will be explored in future work. The S/N of this 2D RFDR spectrum is ~35% of that shown in Fig. 6.

The difference in the behavior of the ^{1}H–^{1}H magnetization exchange under the cross-relaxation (NOE exchange) or the RFDR type mixing periods is more easily understood by measuring the evolution of the ^{1}H–^{1}H exchange as a function of τ_{mix}. To perform multiple ^{1}H–^{13}C INEPT experiments at different τ_{mix} would prove to be extremely time restrictive, but this information can be obtained by using a standard 2D ^{1}H NOESY MAS NMR correlation experiments [13,14,46,49]. From NOESY exchange experiments the individual ^{1}H–^{1}H cross-relaxation rates can be directly measured as shown in Fig. 10 for select protons in the DMPC sample. The results are shown for experiments in which the τ_{mix} contain no rf pulses (standard NOE cross-relaxation) or the dipolar coupling was reintroduced incorporating a ^{1}H RFDR sequence. For protons that are expected to be spatially close the ^{1}H–^{1}H exchange under RFDR is observed to build up very rapidly, reaching a maximum between 10 and 25 ms, followed by a rapid decay away. For example, the exchange between the g_2 and the α protons is extremely rapid, reaching a maximum near 10 ms. The diagonal intensity under the RFDR sequence is also observed to decay much more rapidly than the NOE type cross-relaxation. This decay results from the distribution of the magnetization under RFDR via the recoupled dipolar interactions, but also can be ascribed to a non-recoverable loss of magnetization due to pulse error and timing errors in the multiple-π RFDR pulse train. The performance of the RFDR sequence may be improved by incorporation of additional RFDR phase cycling [54], or the introduction of compensated RFDR sequences [55]. For the NOE based cross-relaxation the buildup rates of the ^{1}H–^{1}H exchange is generally slower (Fig. 10), usually reaching a maximum between 150 and 500 ms as previously noted [13,14,46]. This magnetization exchange occurs through incoherent cross-relaxation which is dependent on both the residual dipolar coupling and the motional correlation time, and scales as r_{ij}^{-6} (where r_{ij} is the ^{1}H–^{1}H distance). The application of the RFDR sequence

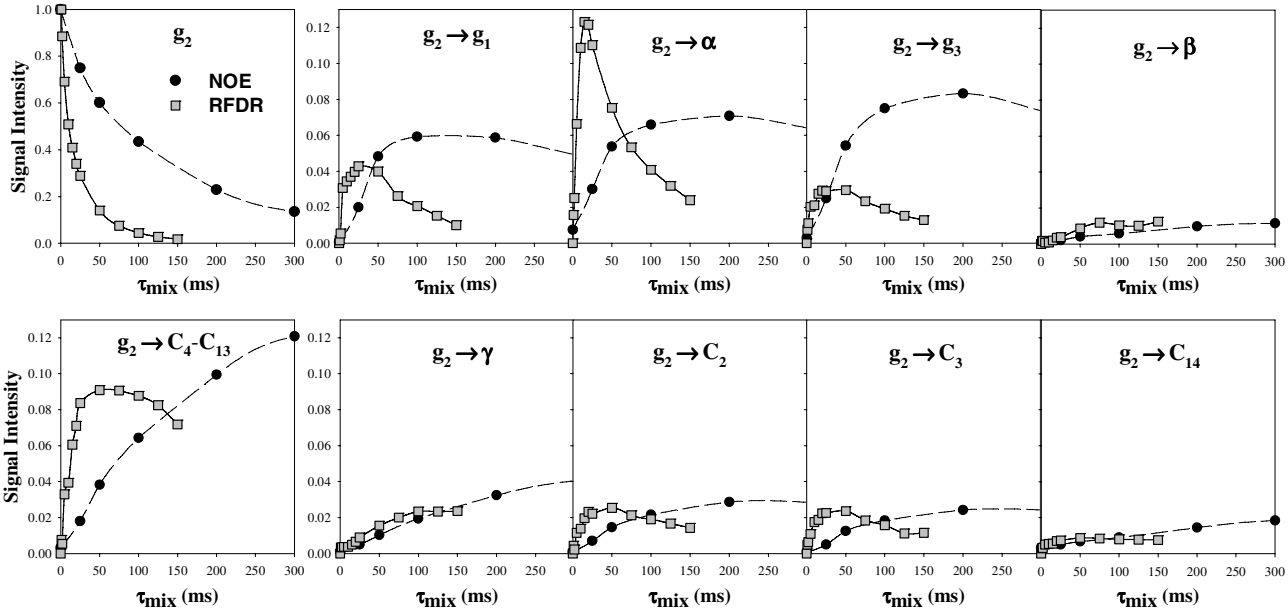

Fig. 10. Selected normalized ^1H–^1H cross peak intensity for the glycerol g_2 proton to other lipid protons obtained from the 2D ^1H–^1H NOESY MAS NMR experiments with NOE cross-relaxation or RFDR recoupling during τ_{mix} for DMPC at 308 K. The cross peaks were normalized to the total intensity of the g_2 diagonal resonance at $\tau_{mix} = 0$.

allows for the recovery (amplification) of dipolar couplings that are averaged by MAS, and not completely averaged by molecular motions. The sequence allows for exchange via a coherent process that is dependent on the reintroduced dipolar coupling independent of the correlation time and will scale as r_{ij}^{-3}. By using short mixing times in the RFDR sequence only protons with a larger (closer) ^1H–^1H dipolar coupling will give rise to exchange, while protons with smaller ^1H–^1H dipolar couplings do not have enough time to buildup and do not exchange. The larger dipolar interactions recoupled under RFDR most likely represent residual intramolecular ^1H–^1H dipolar coupling, since the rapid axial diffusion of the lipids within the membrane are expected to produce a second averaging of dipolar inter-molecular contacts (making them smaller) such that they are not re-introduced by RFDR for short mixing times. By comparing the results of these two exchange experiments it is possible to assign strongly and weakly dipolar coupled protons contacts within membrane systems.

Interestingly, for longer range ^1H–^1H contacts, such as the g_2 proton to the methyl C14 protons (Fig. 10), the magnetization exchange is very similar for the RFDR and the NOE cross- relaxation based experiments. During the RFDR sequence it is known that magnetization transfer can occur both through recoupling and through NOE cross relaxation [49]. It has also been observed that the RFDR sequence may actually accelerate the incoherent NOE cross-relaxation by a process that has been called rotor-driven or RF-driven spin diffusion [56,57]. This type of acceleration of the ^1H–^1H NOE cross-relaxation was not observed for the membrane systems investigated. Further analysis of the individual ^1H–^1H exchange patterns within the complete lipid spin system will be explored in a later manuscript.

It should be noted that the RFDR sequence is not the only dipolar recoupling sequence (or perhaps even the most suitable) that could be utilized during the mixing period of the INEPT sequence shown in Fig. 1. We have also explored the use of the symmetry based double quantum sequence recently described by Levitt and co-workers [58]. For example we have performed ^1H–^{13}C INEPT exchange experiments using the $C7_2^1$ recoupling sequence, and combined $C7_2^1 - C9_3^1$ schemes [59,60], on a lower magnetic field strength instrument observing very similar results (albeit lower resolution) with the nearest neighbor dipolar contacts dominating. Unfortunately the performance of these windowless CN_n^ν -type decoupling sequences [58] on our higher field 600 MHz NMR instrument was rather poor due to hardware limitations and were not pursued further.

4. Conclusions

In conclusion, we have demonstrated a 2D ^1H–^{13}C INEPT correlation experiment for membrane systems. By incorporating a mixing period for ^1H–^1H magnetization exchange structural information can be obtained through the ^{13}C detection of ^1H–^1H contacts. A comparison of the ^1H–^1H correlations observed under a mixing period incorporating NOE cross-relaxation versus correlations observed under the RFDR sequence makes it is possible to identify close intra-molecular ^1H–^1H contacts (or very strong inter-molecular contacts), versus long-range inter-molecular contacts within the membrane constituents. These types of correlation experiments should prove valu-

able for future investigations of complex biomembrane systems.

Acknowledgments

Sandia is a multiprogram laboratory operated by Sandia Corporation, a Lockheed Martin Company, for the United States Department of Energy's National Nuclear Security Administration under Contract DE-AC04-94AL85000. This work is entirely supported by the Sandia LDRD program.

References

[1] K. Gawrisch, N.V. Eldho, I.V. Polozov, Novel NMR tools to study structure and dynamics of biomembranes, Chem. Phys. Lipids 116 (2002) 135–151.
[2] H.C. Gaede, K. Gawrisch, Multi-dimensional pulsed field gradient magic angle spinning NMR experiments on membranes, Magn. Reson. Chem. 42 (2004) 115–122.
[3] F. Lindström, P.T.F. Williamson, G. Gröbner, Molecular insight into the electrostatic membrane surface potential by $^{14}N/^{31}P$ MAS NMR spectroscopy: nociceptin–lipid association, J. Am. Chem. Soc. 127 (2005) 6610–6616.
[4] C. Glaubitz, A. Watts, Magic angle-oriented sample spinning (MAOSS): a new approach towards biomembrane studies, J. Magn. Reson. 130 (1998) 305–316.
[5] J.A. Urbina, E. Oldfield, in: P.I. Harris, D. Chapman (Eds.), Biomembrane Structures, Vol. 20, IOS Press, Washington, DC, 1998, pp. 113–133.
[6] D.E. Warschawski, P.F. Devaux, Polarization transfer in lipid membranes, J. Magn. Reson. 145 (2000) 367–372.
[7] O. Soubias, V. Réat, O. Saurel, A. Milon, High resolution 2D $^{1}H–^{13}C$ correlation of cholesterol in model membrane, J. Magn. Reson. 158 (2002) 143–148.
[8] M. Hong, K. Schmidt-Rohr, D. Nanz, Study of phospholipid structure by ^{1}H, ^{13}C, and ^{31}P dipolar couplings from two-dimensional NMR, Biophys. J. 69 (1995) 1939–1950.
[9] J. Forbes, C. Husted, E. Oldfield, High-filed, high resolution proton "Magic-Angle" sample-spinning nuclear magnetic resonance spectroscopic studies of gel and liquid crystalline lipid bilayers and the effects of cholesterol, J. Am. Chem. Soc. 110 (1988) 1059–1065.
[10] J. Forbes, J. Bowers, X. Shan, L. Moran, E. Oldfield, M.A. Moscarello, Some recent developments in solid-state nuclear magnetic resonance spectroscopic studies of lipids and biological membranes, including the effects of cholesterol in model and natural systems, J. Chem. Soc. Faraday Trans. 1 (84) (1988) 3821–3849.
[11] E. Oldfield, J. Bowers, J. Forbes, High-resolution proton and carbon-13 NMR of membranes: why sonicate, Biochemistry 26 (1987) 6919–6923.
[12] D.E. Warschawski, P.F. Devaux, $^{1}H–^{13}C$ polarization transfer in membranes: a tool for probing lipid dynamics and the effect of cholesterol, J. Magn. Reson. 177 (2005) 166–171.
[13] D. Huster, K. Gawrisch, NOESY NMR crosspeaks between lipid headgroups and hydrocarbon chains: spin diffusion or molecular disorder? J. Am. Chem. Soc. 121 (1999) 1992–1993.
[14] D. Huster, K. Arnold, K. Gawrisch, Investigation of lipid organization in biological membranes by two-dimensional nuclear overhauser enhancement spectroscopy, J. Phys. Chem. B. 103 (1999) 243–251.
[15] L.L. Holte, K. Gawrisch, Determining ethanol distribution in phospholipid multilayers with MAS-NOESY spectra, Biochemistry 36 (1997) 4669–4674.
[16] D. Huster, K. Arnold, K. Gawrisch, Influence of docosahexaenoic acid and cholesterol on lateral lipid organization in phospholipid mixtures, Biochemistry 37 (1998) 17299–17308.
[17] W.-M. Yau, K. Gawrisch, Later lipid diffusion dominates NOESY cross-relaxation in membranes, J. Am. Chem. Soc. 122 (2000) 3971–3972.
[18] S.E. Feller, C.A. Brown, D.T. Nizza, K. Gawrisch, Nuclear overhauser enhancement spectroscopy cross-relaxation rates and ethanol distribution across membranes, Biophys. J. 82 (2002) 1396–1404.
[19] Z.-j. Chen, R.E. Stark, Evaluation spin diffusion in MAS-NOESY spectra of phospholipid multibilayers, Solid State Nucl. Magn. Reson. 7 (1996) 239–246.
[20] N.E. Gabriel, M.F. Roberts, Short-chain lecithin/long-chain phospholipid unilamellar vesicles: asymmetry, dynamics, and enzymatic hydrolysis of the short-chain component, Biochemistry 26 (1987) 2432–2440.
[21] G. Orädd, P.W. Westerman, G. Lindblom, Lateral diffusion coefficients of separate lipid species in a ternary raft-forming bilayer: a PFG-NMR multinuclear study, Biophys. J. 89 (2005) 315–320.
[22] I.V. Polozov, K. Gawrisch, Domains in binary SOPC/POPE lipid mixtures studied by pulse field gradient ^{1}H MAS NMR, Biophys. J. 87 (2004) 1741–1751.
[23] A. Pampel, K. Zick, H. Glauner, F. Engelke, Studying lateral diffusion in lipid layers by combining a magic angle spinning NMR probe with a microimaging gradient system, J. Am. Chem. Soc. 126 (2004) 9534–9535.
[24] O. Soubias, K. Gawrisch, Probing specific lipid–protein interaction by saturation transfer difference NMR spectroscopy, J. Am. Chem. Soc. 127 (2005) 13110–13111.
[25] M. Hong, K. Schmidt-Rohr, H. Zimmermann, Conformational constraints on the headgroup and *sn*-2 chain of bilayer DMPC from NMR dipolar couplings, Biochemistry 35 (1996) 8335–8341.
[26] S. Everts, J.H. Davies, ^{1}H and ^{13}C NMR of multilamellar dispersions of polyunsaturated (22;6) phospholipids, Biophys. J. 79 (2000) 885–897.
[27] C.W.B. Lee, R.G. Griffin, Two-dimensional $^{1}H/^{13}C$ heteronuclear chemical shift correlation spectroscopy of lipid bilayers, Biophys. J. 55 (1989) 355–358.
[28] J.D. Gross, D.E. Warschawski, R.G. Griffin, Dipolar recoupling in MAS NMR: a probe for segmental order in lipid bilayers, J. Am. Chem. Soc. 119 (1997) 796–802.
[29] S.V. Dvinskikh, V. Castro, D. Sandström, Efficient solid-state NMR methods for measuring heteronuclear dipolar couplings in unoriented lipid membrane systems, Phys. Chem. Chem. Phys. 7 (2005) 607–613.
[30] J.A. Urbina, B. Moreno, W. Arnold, C.H. Taron, P. Orlean, E. Oldfield, A carbon-13 nuclear magnetic resonance spectroscopic study of inter-proton order parameters: a new approach to study order and dynamics in phospholipid membrane systems, Biophys. J. 75 (1998) 1372–1383.
[31] J.D. Gross, P.R. Costa, J.-P. Dubacq, D.E. Warschawaski, P.-N. Lirsac, P.F. Devaux, R.G. Griffin, Multidimensional NMR in lipid systems. coherence transfer through J couplings under MAS, J. Magn. Reson. B 106 (1995) 187–190.
[32] O. Soubias, M. Piotto, O. Saurel, O. Assemat, V. Réat, A. Milon, Detection of natural abundance $^{1}H–^{13}C$ correlations of cholesterol in its membrane environment using a gradient enhanced HSQC experiment under high resolution magic angle spinning, J. Magn. Reson. 165 (2003) 303–308.
[33] O. Soubias, F. Jolibois, V. Réat, A. Milon, Understanding sterol-membrane interactions, Part II: Complete ^{1}H and ^{13}C assignments by solid-state spectroscopy and determination of the hydrogen-bonding partners of cholesterol in a lipid bilayer, Chem. Eur. J. 10 (2004) 6005–6014.
[34] B. Alonso, D. Massiot, Multi-scale NMR characterization of meso-structured materials using $^{1}H–^{13}C$ through-bond polarization transfer, fast MAS, and ^{1}H spin diffusion, J. Magn. Reson. 163 (2003) 347–352.
[35] S.V. Dvinskikh, V. Castro, D. Sandström, Heating caused by radiofrequency irradiation and sample rotation in ^{13}C magic angle spinning NMR studies of lipid membranes, Magn. Reson. Chem. 42 (2004) 875–881.
[36] D.J. States, R.A. Haberkorn, D.J. Ruben, A two-dimensional nuclear overhauser experiment with pure adsorption phase in four quadrants, J. Magn. Reson. 48 (1982) 286–292.

[37] D.K. Sodickson, M.H. Levitt, S. Vega, R.G. Griffin, Broad band dipolar recoupling in the nuclear magnetic resonance of rotating solids, J. Chem. Phys. 98 (1993) 6742–6748.
[38] A.E. Bennett, J.H. Ok, R.G. Griffin, S. Vega, Chemical shift correlation spectroscopy in rotating solids: radio frequency-driven dipolar recoupling and longitudinal exchange, J. Chem. Phys. 96 (1992) 8624–8627.
[39] C. Jäger, M. Feike, R. Born, H.W. Spiess, Direct detection of connectivities in glasses by 2D NMR, J. Non-Cryst. Solids 180 (1994) 91–95.
[40] A.E. Bennett, C.M. Rienstra, M. Auger, K.V. Lakshmi, R.G. Griffin, J. Chem. Phys. 103 (1995) 6951–6958.
[41] W. Guo, J.A. Hamilton, A multinuclear solid-state NMR study of phospholipid–cholesterol interactions. Dipalmitoylphosphatidylcholine–cholesterol binary system, Biochemistry 34 (1995) 14174–14184.
[42] M.R. Vist, J.H. Davis, Phase equilibria of cholesterol/dipalmotoylphosphatidylcholine mixtures: 2H nuclear magnetic resonance and differential scanning calorimetry, Biochemistry 29 (1990) 451–464.
[43] J.H. Ipsen, G. Karlström, O.G. Mouritsen, H. Wennerström, M.J. Zuckermann, Phase equilibrium in the phosphatidyl–cholesterol system, Biochim. Biophys. Acta 905 (1987) 162–172.
[44] T.P. Trouard, A.A. Nevzorov, T.M. Alam, C. Job, J. Zajicek, M.F. Brown, Influence of cholesterol on dynamics of dimyristoylphosphatidylcholine bilayers as studied by deuterium NMR relaxation, J. Chem. Phys. 110 (1999) 8802–8818.
[45] K.V. Schenker, v. Philipsborn, Optimization of INEPT and DEPT experiments for spin systems with hetero- and homonuclear couplings, J. Magn. Reson. 61 (1985) 294–305.
[46] D. Huster, X. Yao, M. Hong, Membrane protein topology probed by ^{1}H spin diffusion from lipids using solid state NMR spectroscopy, J. Am. Chem. Soc. 124 (2002) 874–883.
[47] A.E. Bennett, C.M. Rienstra, J.M. Griffiths, W. Zhen, P.T. Lansbury, R.G. Griffin, Homonuclear radio frequency-driven recoupling in rotating solids, J. Chem. Phys. 108 (1998) 9463–9479.
[48] H. Geen, J. Gottwald, R. Graf, I. Schnell, H.W. Spiess, J.J. Titman, Elucidation of dipolar coupling networks under magic-angle spinning, J. Magn. Reson. 125 (1997) 224–227.
[49] J. Raya, A. Bianco, J. Furrer, J.-P. Briand, M. Piotto, K. Elbayed, Proton dipolar recoupling in resin-bound peptides under high-resolution magic angle spinning, J. Magn. Reson. 157 (2002) 43–51.
[50] A. Lange, S. Luca, M. Baldus, Structural constraints from proton mediated rare-spin correlation spectroscopy in rotating solids, J. Am. Chem. Soc. 2002 (2002) 9704–9705.
[51] Y. Matsuki, H. Akutsu, T. Fujiwara, Precision ^{1}H–^{1}H distance measurement via ^{13}C NMR signals: utilization of ^{1}H–^{1}H double quantum dipolar interactions recoupled under magic angle spinning conditions, Magn. Reson. Chem. 42 (2004) 291–300.
[52] B. Reif, C.P. Jaroniec, C.M. Tienstra, M. Hohwy, R.G. Griffin, ^{1}H–^{1}H MAS correlation spectroscopy and distance measurements in a deuterated peptide, J. Magn. Reson. 151 (2001) 320–327.
[53] B. Reif, R.G. Griffin, ^{1}H detected ^{1}H, ^{15}N correlation spectroscopy in rotating solids, J. Magn. Reson. 160 (2003) 78–83.
[54] T. Gullion, D.B. Baker, M.S. Conradi, New, compensated Carr–Purcell sequences, J. Magn. Reson. 89 (1990) 479–484.
[55] T. Fujiwara, P. Khandelwal, H. Akutsu, Compound radio-frequency-driven Recoupling pulse sequences for efficient magnetization transfer by homonuclear dipolar interactions under magic-angle spinning conditions, J. Magn. Reson. 145 (2000) 73–83.
[56] P. Robyr, B.H. Meier, R.R. Ernst, Radio-frequency-driven nuclear spin diffusion in solids, Chem. Phys. Lett. 162 (1989) 417.
[57] M.G. Colombo, B.H. Meier, R.R. Ernst, Rotor-driven spin diffusion in natural abundance ^{13}C spin systems, Chem. Phys. Lett. 146 (1988) 189–196.
[58] A. Brinlmann, M. Edén, M.H. Levitt, Synchronous helical pulse sequences in magic-angle spinning nuclear magnetic resonance: Double quantum recoupling of multiple-spin systems, J. Chem. Phys. 112 (2000) 8539–8554.
[59] K. Thieme, G. Zech, H. Kunz, H.W. Spiess, I. Schnell, Dipolar recoupling in NOESY-type ^{1}H–^{1}H NMR experiments under HRMAS conditions, Org. Lett. 4 (2002) 1559–1562.
[60] I. Schnell, Merging concepts from liquid-state and solid-state NMR spectroscopy for the investigation of supra- and biomolecular systems, Curr. Anal. Chem. 1 (2005) 3–27.